

Chemical Imaging with Combined Fast-Scan Cyclic Voltammetry–Scanning Electrochemical Microscopy

Daniel S. Schrock[†] and John E. Baur^{*}

Department of Chemistry, Illinois State University, Normal, Illinois 61790–4160

Fast-scan cyclic voltammetry (FSCV) is applied to the tip of a scanning electrochemical microscope (SECM) for imaging the distribution of chemical species near a substrate. This approach was used to image the diffusion layer of both a large substrate electrode (3-mm-diameter glassy carbon) and a microelectrode substrate (10- μ m-diameter Pt). Additionally, oxygen depletion near living cells was measured and correlated to respiratory activity. Finally, oxygen and hydrogen peroxide were simultaneously detected during the oxidative burst of a zymosan-stimulated macrophage cell. These results demonstrate the utility of FSCV–SECM for chemical imaging when conditions are chosen such that feedback interactions with the substrate are minimal.

The recent combination of fast-scan cyclic voltammetry (FSCV) with scanning electrochemical microscopy (SECM) has produced a new multidimensional technique for the investigation of chemical processes occurring at interfaces.^{1,2} In this technique, cyclic voltammetry is carried out at the SECM tip at rapid scan rates, typically between 10 and 1000 V·s^{−1}. Four-dimensional data sets are produced for imaging experiments (*I* vs *E* at each *xy* or *xd* location), and three-dimensional data sets are produced for approach curves or line scans (*I* vs *E* at each *d* or *x* position). Electroactive species having different redox potentials are measured with each cyclic voltammogram, and therefore, FSCV–SECM can simultaneously detect multiple species with micrometer spatial resolution. Chemical images of a selected species can be extracted from the four-dimensional data set by plotting current measured at the appropriate tip potential as a function of *xy* position.

With FSCV, electrolyzed products are generated only transiently, and for chemically reversible redox systems, most of the electrolyzed product is returned to its initial state during the reverse sweep. As a result, there is very little redox product generated that can interact with the substrate. For biological systems, this is particularly advantageous compared to conventional SECM where the tip is held at a constant potential, continuously generating electrolysis products. Such byproducts

are potentially stimulatory, inhibitory, or even toxic to biological substrates. Furthermore, with FSCV, the diffusion layer does not extend far from the tip surface.³ As a result, the tip can be brought much closer to a substrate without encountering the positive or negative feedback effects typically observed with conventional SECM.^{4,5} For these reasons, FSCV–SECM promises to be more amenable to measurements in biological systems than conventional SECM.

FSCV–SECM was first introduced by Wipf.¹ In that work, the instrumentation was detailed, and varied applications of the technique were introduced. In all but one of these applications, the imaging was dependent upon the addition of a redox mediator to the electrochemical cell. The application not requiring the addition of a mediator involved the measurement of chloride ion in an acidic medium by stripping voltammetry at a mercury SECM tip. Since our interests lie in chemical imaging in biological systems, we wish to extend the work of Wipf and apply FSCV–SECM to the chemical imaging of endogenous species under biologically relevant conditions (i.e., neutral pH and physiological ionic strengths).

We recently described the conditions under which feedback interactions with conductive and insulating substrates can be avoided when using FSCV–SECM.² Briefly, faster voltammetric scan rates, *v*, or increased tip–substrate separation distances, *d*, can greatly reduce diffusional interactions between the tip and substrate. For example, at *v* = 1000 V·s^{−1}, feedback effects were absent at *d* = 1 μ m (7- μ m-diameter tip electrode) and nearly absent at *v* = 100 V·s^{−1} and *d* = 3 μ m. When investigating these feedback effects in the previous work, it was necessary to add a redox mediator to the electrochemical cell. The aim of the present article is to describe the use of FSCV–SECM for substrate generator–tip collector (SG–TC) measurements in systems having no added mediator and under conditions where feedback interactions do not occur or are negligible. For all experiments, the SECM tip is a carbon fiber electrode, which is particularly well-suited for FSCV in biological systems.⁶

^{*} Corresponding author. Fax: (309)438-5538. E-mail: jebaur@ilstu.edu.

[†] Present address: Abbott Molecular, Des Plaines, IL 60018.

(1) Díaz-Ballote, L.; Alpuche-Aviles, M.; Wipf, D. O. *J. Electroanal. Chem.* **2007**, *604*, 17–25.

(2) Schrock, D. S.; Wipf, D. O.; Baur, J. E. *Anal. Chem.* **2007**, *79*, 4931–4941.

(3) Wightman, R. M.; Wipf, D. O. In *Electroanalytical Chemistry*; Bard, A. J., Ed.; Marcel Dekker, Inc.: New York, 1989; Vol. 15, pp 267–352.

(4) Bard, A. J.; Fan, F.-R. F.; Mirkin, M. V. In *Electroanalytical Chemistry*; Bard, A. J., Ed.; Marcel Dekker: New York, 1994; Vol. 18, pp 243–373.

(5) Kwak, J.; Bard, A. J. *Anal. Chem.* **1989**, *61*, 1221–1227.

(6) Wightman, R. M.; May, L. J.; Michael, A. *Anal. Chem.* **1988**, *60*, 769A–779A.

Initially, vertical concentration gradients (i.e., diffusion layer profiles) are measured with FSCV at a large substrate electrode (planar diffusion) and at a microelectrode substrate (convergent diffusion). These experimental diffusion layer profiles are compared to theory for each case. Engstrom first reported the use of a microelectrode to probe the diffusion layer near a large substrate electrode 20 years ago.^{7,8} In some of that work, the probe was switched off between measurements to prevent redox cycling (i.e., positive feedback) between the probe and substrate, ensuring that the measurement of the diffusion layer was essentially SG–TC. In essence, the use of FSCV–SECM is an analogous but somewhat more sophisticated approach; the cyclic voltammogram provides more information than can be obtained at a constant tip potential, and a rest potential can be chosen such that during the delay between scans there is no tip–substrate interaction. Furthermore, even during acquisition of the voltammogram, the diffusion layer is small enough that there are no diffusional interactions except at very low values of d .

Next, we measure concentration gradients generated by living cells using a voltammetric waveform developed for the simultaneous detection of dopamine, oxygen, and pH.^{9,10} We have applied this technique to two different biological systems. In the first, we image oxygen consumption by PC12 cells, a model system for neuronal function. PC12 cells have been used for several studies with the SECM.^{11–15} Matsue demonstrated that oxygen consumed by these cells can be detected and is a useful measure of cell respiration.¹⁵ In that work, oxygen was detected by reduction at a Pt tip. However, detection of oxygen by continuous reduction is potentially disadvantageous because it consumes available oxygen, further diminishing the solution oxygen concentration near the cell. It can also produce an acidic pH change if the solution is not well-buffered. At least transiently, oxygen reduction also can produce reactive species such as hydrogen peroxide. Each of these might have consequences for the cell's viability, thus limiting the usefulness of the technique, especially for long-term imaging. Furthermore, with constant-potential SECM, the signal is susceptible to negative feedback effects, and hence, the chemical image is inextricably linked to substrate topography. With FSCV–SECM, each of these disadvantages is overcome. The generation of redox products is greatly diminished because of the only momentary reduction of oxygen; with the waveform used for voltammetry, oxygen is reduced only ~2.5% of the time. By operating at voltammetric scan rates where feedback effects are absent,² measured current is only a function of analyte concentra-

tion at the tip location, and therefore, topography becomes less of a concern. These factors, combined with the fact that the response of carbon fibers to oxygen is very stable when using FSCV,¹⁶ suggest that the technique will be well-suited to oxygen imaging with a cellular substrate.

In the second cellular system, RAW 264.7 macrophages are used as a model biological substrate in which more than one chemical species can be imaged. These cells produce an oxidative burst upon immunological stimulation with a substance such as zymosan. Among the species typically generated by the macrophage during the oxidative burst is hydrogen peroxide, a species that is detectable using the same waveform as used for detection of oxygen. With FSCV–SECM, we can simultaneously image oxygen, hydrogen peroxide, and an unidentified species related to the oxidative burst.

EXPERIMENTAL SECTION

Instrumental Methods. The instrument used for FSCV–SECM was based on that described previously,² except that an external arbitrary waveform generator (model 33220A, Agilent Technologies, Santa Clara, CA) was used to generate the potential waveform for cyclic voltammetry instead of the bipotentiostat's internal triangle wave generator. Stimulant solutions were delivered focally by pressure ejection at 10–20 psi from a micropipet (~3–7 μm in diameter) using a PicoSpritzer II (General Valve Corp., Fairfield, NJ). Data were collected with a custom software package provided by Dr. David Wipf of Mississippi State University. The image data (I vs E vs xy or xd position) was processed using the CITS module of the scanning probe image processor (Image Metrology, Lyngby, Denmark). This software allows for the extraction of voltammograms at specific xy or xd locations and the selection of images (I vs xy or xd) at a specified tip potential. When multiple images were averaged over a potential range, locally written software was used to extract the data and save it in the CITS format. A single Gaussian smooth was applied to images recorded at the fastest voltammetric scan rates (450 and 1000 $\text{V}\cdot\text{s}^{-1}$) to improve the signal-to-noise ratio.

The reported tip–substrate distances (d) were found by first lowering the probe electrode until it contacted the substrate ($d = 0$) and then raising the probe the appropriate distance. In solutions of 4-aminoTEMPO, contact with the substrate was determined by monitoring the positive feedback signal with the substrate potential set at 0.0 V and the tip potential set at +0.8 V. In all other solutions, contact with the substrate was detected from the negative feedback of dissolved O_2 using a tip potential of –1.2 V.

Comsol Multiphysics (Version 3.3, Comsol, Inc., Burlington, MA) was used to simulate the diffusion layer of a microelectrode substrate. These calculations were done in two dimensions using the steady-state diffusion application mode and axial symmetry. Weak restraints were employed to improve the accuracy of the calculation at the electrode surface. Adaptive mesh refinement (a total of 10 refinements) was used to improve the mesh quality; the final mesh consisted of 7400 elements.

Electrodes. All tips used for the SECM were made from 7- μm -diameter carbon fibers (Thornel T-650, Cytec, Greenville, SC) sealed in glass capillaries and polished at 90° on a micropipet

- (7) Engstrom, R. C.; Meaney, T.; Tople, R.; Wightman, R. M. *Anal. Chem.* **1987**, *59*, 2005–2010.
- (8) Engstrom, R. C.; Weber, M.; Wunder, D. J.; Burgess, R.; Wingquist, S. *Anal. Chem.* **1986**, *58*, 844–848.
- (9) Michael, D.; Travis, E. R.; Wightman, R. M. *Anal. Chem.* **1998**, *70*, 586A–592A.
- (10) Venton, B. J.; Michael, D. J.; Wightman, R. M. *J. Neurochem.* **2003**, *84*, 373–381.
- (11) Kurulugama, R. T.; Wipf, D. O.; Takacs, S. A.; Pongmayteegul, S.; Garriss, P. A.; Baur, J. E. *Anal. Chem.* **2005**, *77*, 1111–1117.
- (12) Liebetrau, J. M.; Miller, H. M.; Baur, J. E.; Takacs, S. A.; Anupunpisit, V.; Garriss, P. A.; Wipf, D. O. *Anal. Chem.* **2003**, *75*, 563–571.
- (13) Maruyama, K.; Ohkawa, H.; Ogawa, S.; Ueda, A.; Niwa, O.; Suzuki, K. *Anal. Chem.* **2006**, *78*, 1904–1912.
- (14) Takahashi, Y.; Hirano, Y.; Yasukawa, T.; Shiku, H.; Yamada, H.; Matsue, T. *Langmuir* **2006**, *22*, 10299–10306.
- (15) Takii, Y.; Takoh, K.; Nishizawa, M.; Matsue, T. *Electrochim. Acta* **2003**, *48*, 3381–3385.

- (16) Zimmerman, J. B.; Wightman, R. M. *Anal. Chem.* **1991**, *63*, 24–28.

beveller (BV-10, Sutter Instruments, Novato, CA).¹⁷ Only electrodes having an overall diameter of 10 μm or less (corresponding to $\text{RG} \leq 1.5$) were used. For experiments involving oxygen, hydrogen peroxide, and pH, the carbon fiber electrode was postcalibrated to determine the quantitative relationship between peak current and analyte concentration. A flow system having a pneumatically activated loop injector was used for this calibration. When calibrating the oxygen response, a flow system having stainless steel tubing was used to prevent atmospheric oxygen from permeating the tubing and altering the oxygen concentration in the calibrant solution. For pH and hydrogen peroxide calibrations, a flow system with Teflon tubing was used. All potentials are reported versus a 3 M Ag/AgCl reference electrode.

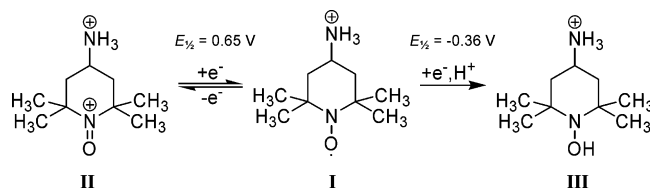
Reagents. Solutions of 4-aminoTEMPO (Aldrich, St. Louis, MO) were prepared in a 0.1 M pH 7.4 phosphate buffer. To prevent interference from the reduction of dissolved oxygen at the substrate electrode, solutions of 4-aminoTEMPO were deoxygenated prior to use, and the SECM cell was blanketed with nitrogen during imaging experiments. Hank's buffer (Sigma, St. Louis, MO) with added HEPES (10 mM) was used for imaging biological cells and for postcalibration of the electrodes. All solutions were prepared with deionized water (NanoPure, Barnstead-Thermolyne, Inc., Dubuque, IA).

Cell Culture. RAW 264.7 cells (ATCC, Manassas, VA) were maintained at 37 $^{\circ}\text{C}$ (5% CO_2) in Dulbecco's Modification of Eagle's Serum (Sigma) supplemented with 10% fetal calf serum (Atlanta Biologicals, Norcross, GA), L-glutamine, and penicillin–streptomycin antibiotics (Sigma). At least 24 h prior to use, the cells were plated on uncoated polystyrene tissue culture plates and returned to the incubator. Stimulant solutions for RAW 264.7 cells were prepared by suspending zymosan A from *Saccharomyces cerevisiae* (Sigma) in sterile saline solution to yield a 50 mg/mL suspension. Three volumes of mouse serum (Harlan Bioproducts, Indianapolis, IN) were added, and the suspension was incubated at 37 $^{\circ}\text{C}$ for 30 min. Following centrifugation, the serum was decanted and the opsonized zymosan was resuspended in sterilized phosphate-buffered saline.

PC12 cells (ATCC) were maintained at 37 $^{\circ}\text{C}$ (5% CO_2) in RPMI-1640 growth media (Sigma) supplemented with 10% donor horse serum, 5% fetal bovine serum (Atlanta Biologicals), and penicillin–streptomycin antibiotics. The cells were plated on collagen-coated polystyrene tissue culture plates and incubated for at least 2 days prior to use. Stimulant solutions for the PC12 cells consisted of a modified Hank's buffer in which K^+ replaced Na^+ on a 1:1 molar basis so that the final concentration of K^+ was 100 mM.

RESULTS AND DISCUSSION

Diffusion Layer Imaging. Initially, concentration gradients were generated by a substrate electrode reducing 4-aminoTEMPO (**I**, TEMPO = 2,2,6,6-tetramethylpiperidine 1-oxyl). This stable free radical undergoes a reversible oxidation to an oxoammonium ion (**II**) and an irreversible reduction to a hydroxylamine (**III**):^{18–20}



At neutral pH the amino group is protonated and thus each redox form has a net positive charge. With the substrate set to irreversibly reduce the free radical, FSCV was used to interrogate the free-radical concentration in solution via the reversible oxidation reaction.

Figure 1 shows the diffusion layer of a 3-mm-diameter glassy carbon substrate electrode recorded with FSCV–SECM. These approach surfaces (change in current, i , plotted as a function of potential, E , and tip–substrate separation, d) were recorded at three voltammetric scan rates (10, 100, and 1000 $\text{V}\cdot\text{s}^{-1}$). The electrochemical cell contained a deoxygenated solution of 1.0 mM 4-aminoTEMPO free radical (**I**), and the substrate potential was held at -1.0 V , causing the irreversible reduction of the radical to the hydroxylamine (**III**). The potential of the carbon fiber tip was scanned from 0.0 to $+1.0 \text{ V}$, reversibly oxidizing the free radical to the oxoammonium ion (**II**) and back to the free radical. The current measured by the tip voltammogram is thus a measure of the concentration of the free radical at the tip location. Because the free radical is quickly regenerated on the reverse sweep, the overall concentration of free radical in the substrate diffusion layer should not be significantly perturbed by the measurement. The approach surfaces show that the anodic peak is shifted to more positive potentials at faster voltammetric scan rates, indicative of the quasireversible behavior of 4-aminoTEMPO at the carbon fiber tip. However, the distance dependence of the change in peak current is similar at each voltammetric scan rate, as expected for a TG–SC experiment where the tip does not interfere with the substrate reaction.

Figure 2 shows approach curves extracted from the approach surfaces of Figure 1 at the peak anodic potential and at $+0.3 \text{ V}$ (well below the $E_{1/2}$ of the oxidation reaction) over a vertical distance of 1 mm. The concentration gradient, reported as normalized concentration (C/C^* , where C^* is the concentration of the bulk solution), was calculated by dividing the change in current between $d = 0$ and d by the overall change in current between $d = 0$ and $d = 1000 \mu\text{m}$. For the large substrate electrode, planar diffusion predominates and the vertical concentration gradient should follow the function

$$\frac{C(d,t)}{C^*} = \text{erf}\left[\frac{d}{2(Dt)^{1/2}}\right] \quad (1)$$

where $C(d,t)$ is the concentration at distance d from the substrate at time t and D is the diffusion coefficient.²¹ Also shown in Figure 2 are fits for the concentration gradients using $D = 4.7 \times 10^{-6} \text{ cm}^2\cdot\text{s}^{-1}$ ²² and at t values indicated in the figure caption. Clearly

(17) Kelly, R. S.; Wightman, R. M. *Anal. Chim. Acta* **1986**, *187*, 79–87.

(18) Baur, J. E.; Wang, S.; Brandt, M. C. *Anal. Chem.* **1996**, *68*, 3816–3821.

(19) Fish, J. R.; Swarts, S. G.; Sevilla, M. D.; Malinski, T. J. *Phys. Chem.* **1988**, *92*, 3745–3751.

(20) Morris, S.; Sosnovsky, G.; Hui, B.; Huber, C. O.; Rao, N. U. M.; Swartz, H. M. *J. Pharm. Sci.* **1991**, *80*, 149–152.

(21) Bard, A. J.; Faulkner, L. R. *Electrochemical Methods: Fundamentals and Applications*, 2nd ed.; John Wiley & Sons, Inc.: New York, 2001.

(22) Whited, B. L. M.S. Thesis, Illinois State University, Normal, IL 1996.

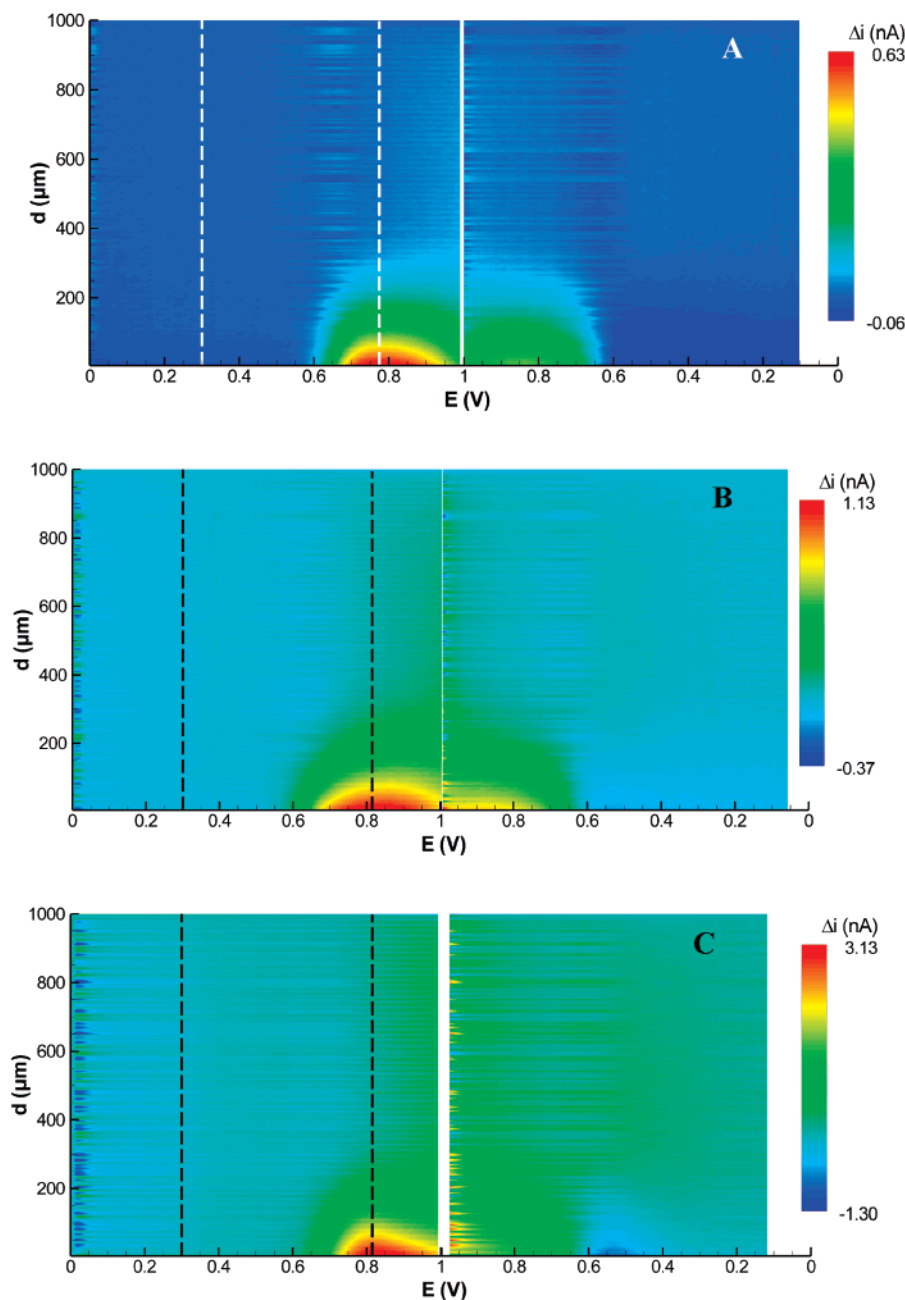


Figure 1. FSCV approach surfaces recorded with a 7- μm -diameter carbon fiber tip and a 3-mm-diameter glassy carbon substrate electrode held at -1.0 V in a deoxygenated solution of 1 mM 4-aminoTEMPO. Tip voltammetric scan rates are (A) 10, (B) 100, and (C) 1000 $\text{V}\cdot\text{s}^{-1}$. The change in current was calculated by subtracting the tip current far from the substrate ($d = 1000\text{ }\mu\text{m}$) from each voltammogram. Because anodic current is taken as negative, an increase in Δi corresponds to a decrease in the magnitude of the anodic current. The tip was brought toward the substrate at a rate of $10\text{ }\mu\text{m}\cdot\text{s}^{-1}$.

the measured concentration gradients follow theory, although there is some ambiguity in assigning the value of t . Because eq 1 shows that the concentration gradient is time-dependent, C/C^* should continually change while the approach curve is recorded. However, the approach surfaces were recorded several minutes after the application of the reducing potential to the substrate, and it is known that at long times natural convection from density gradients, vibrations, etc., limit the actual diffusion layer size.²¹ The values of t used to fit the experimental data are therefore comparable to those expected for an unshielded planar electrode. Furthermore, the presence of the moving tip may have a small influence on the measured diffusion layer. This is perhaps

evidenced by the fact that the concentration gradient is steepest when a voltammetric scan rate of $1000\text{ V}\cdot\text{s}^{-1}$ was used. Although identical z velocities were used for recording the approach surfaces, the effective speed is fastest at $1000\text{ V}\cdot\text{s}^{-1}$ because the tip is stationary while a voltammogram is recorded. At $1000\text{ V}\cdot\text{s}^{-1}$, a voltammogram is recorded in $\sim 2\text{ ms}$, so there is only a negligible delay between tip movements. This higher velocity may account for the small difference in the value of t required to fit the data. Nonetheless, the excellent agreement between the theoretical and measured concentration gradients demonstrates that FSCV-SECM is well-suited to SG-TC measurements. Furthermore, the fact that the concentration gradient closely follows the theory even

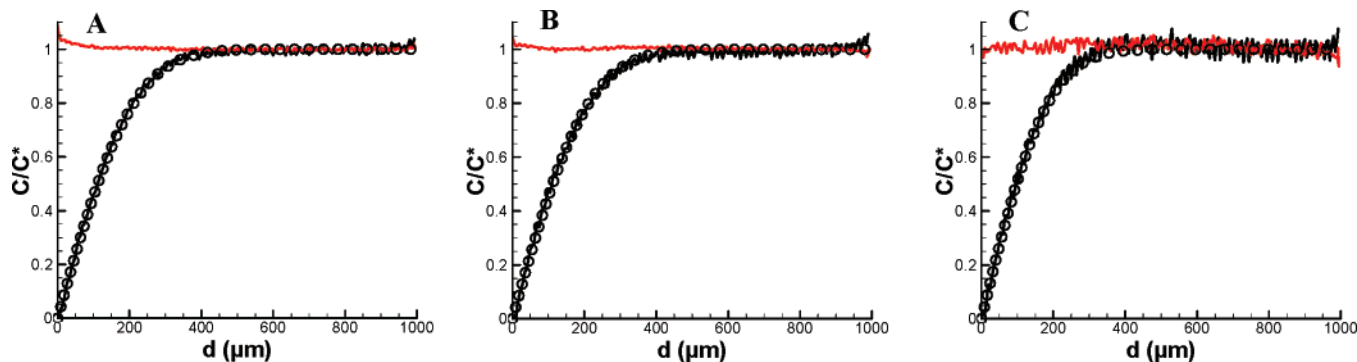


Figure 2. Approach curves extracted from Figure 1 at the potentials indicated by the vertical dashed lines in Figure 1. The red lines were extracted at $E = +0.3$ V (anodic segment), and the black lines were extracted at $E_{p,a}$. The data were recorded at tip voltammetric scan rates of (A) 10, (B) 100, and (C) 1000 $\text{V}\cdot\text{s}^{-1}$. The normalized concentration (C/C^*) was calculated by dividing the background-corrected current at distance d by the current at $d = 1000$ μm . Circles show the calculated concentration gradient for planar diffusion (eq 1) using (A) $t = 25$ s, (B) $t = 25$ s, and (C) $t = 19$ s.

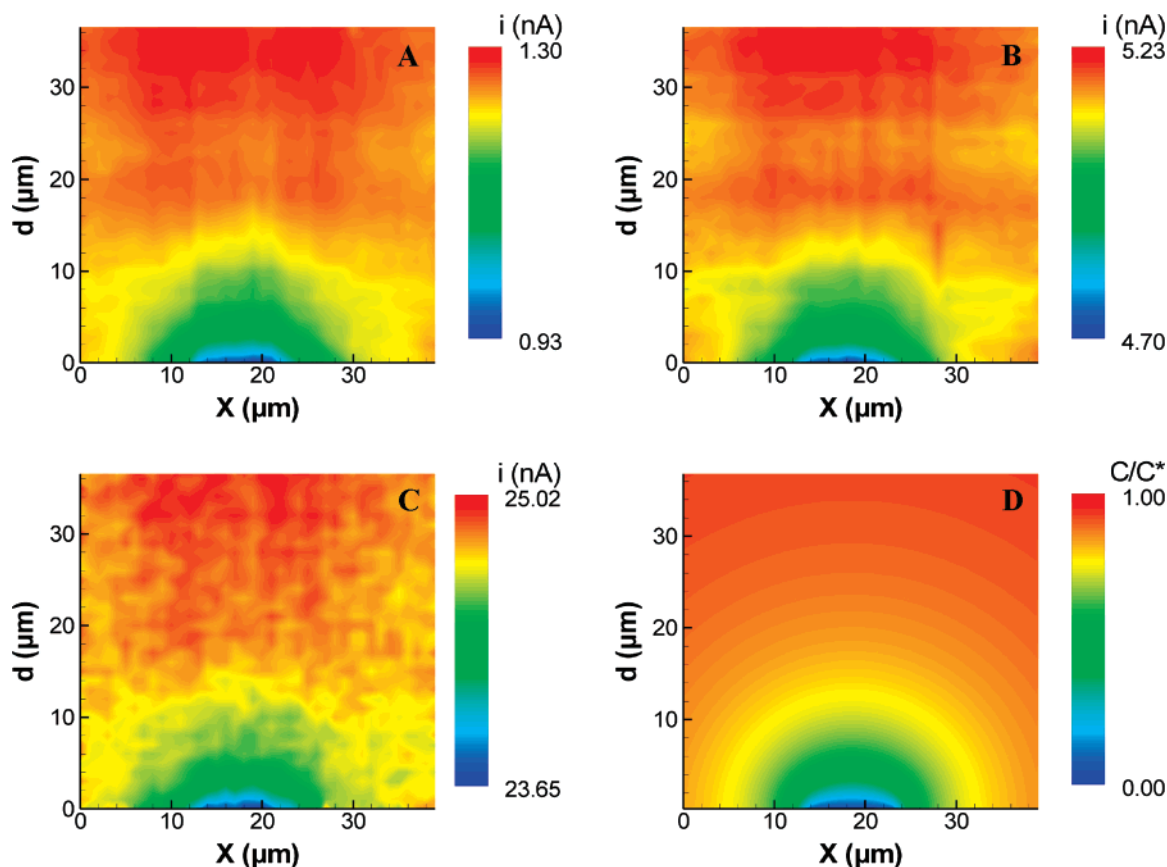


Figure 3. FSCV-based generator-collector images of the diffusion layer above a 10- μm -diameter Pt electrode irreversibly reducing 1.0 mM 4-aminoTEMPO in deoxygenated pH 7.4 phosphate buffer. Tip current was recorded at $E_{p,a}$ for the reversible oxidation of 4-aminoTEMPO at voltammetric scan rates of (A) 10, (B) 100, and (C) 1000 $\text{V}\cdot\text{s}^{-1}$. A simulated steady-state diffusion layer is shown in (D).

as d approaches zero indicates that there are not appreciable amounts of redox products reaching the substrate even at the lowest voltammetric scan rate used (10 $\text{V}\cdot\text{s}^{-1}$).

The diffusion layer of a 10- μm -diameter Pt substrate electrode was imaged in a similar manner except that a series of approach surfaces were recorded across the electrode (x dimension), producing a two-dimensional profile. Figure 3 shows vertical (xd) images of the diffusion layer at the microelectrode substrate recorded at the three different voltammetric scan rates. These images were made by extracting the peak anodic current measured by the tip at each xd location. For comparison, a calculated

diffusion layer for a microelectrode substrate is shown in Figure 3D. Clearly the experimental images closely resemble the theoretical diffusion layer for convergent diffusion at microelectrodes. Additionally, the shapes of the experimentally measured diffusion layers are independent of scan rate, indicating that there were no significant feedback effects present. There is a noticeable decrease in the signal-to-noise ratio with increasing voltammetric scan rate, however. This is a consequence of the fact that the background current increases proportionally with voltammetric scan rate but faradic current increases proportionally with the square root of the scan rate.

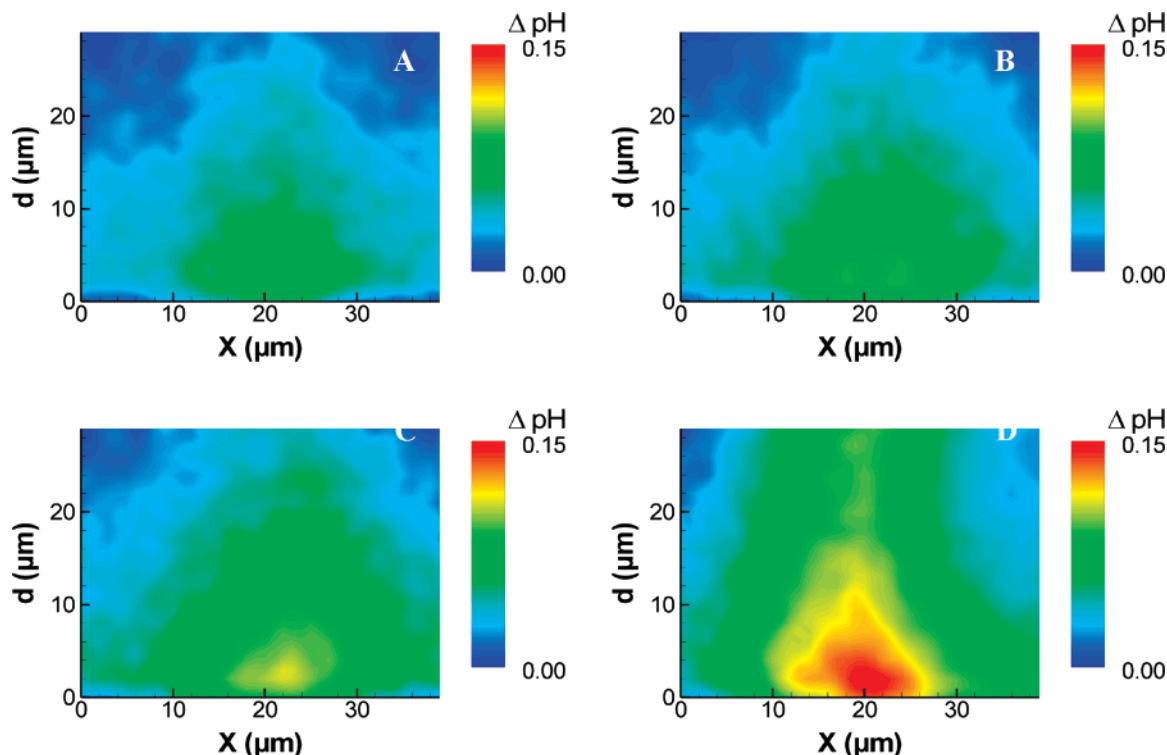


Figure 4. FSCV-based generator–collector images of the pH gradient generated by a 10- μm -diameter Pt electrode reducing H^+ . The potential of the substrate was held at (A) -0.6 , (B) -0.8 , (C) -1.0 , and (D) -1.2 V in a 0.5 mM HEPES buffer containing 150 mM Na^+ . The potential applied to the tip consisted of a three-segment waveform (0.0 to $+1.2$ to -1.4 to 0.0 V) having a scan rate of $450 \text{ V}\cdot\text{s}^{-1}$. The measured current, averaged over 5 potentials between -0.24 and -0.28 V on the final anodic segment, was converted to pH using postcalibration data.

FSCV–SECM is also capable of imaging diffusion layers in solutions without added electroactive species. The background current at carbon fiber electrodes is sensitive to changes in pH over a limited range when using FSCV.^{10,23} This sensitivity to pH arises from changes in the carbon surface redox waves, not directly from reduction of protons. It is possible to use this background change to image pH gradients generated by a substrate electrode. Figure 4 shows vertical pH gradients created by a 10- μm -diameter Pt substrate electrode held at sufficiently negative potentials to reduce H^+ . To detect pH changes, the tip potential was scanned from 0.0 to $+1.2$ to -1.4 back to 0.0 V at a scan rate of $450 \text{ V}\cdot\text{s}^{-1}$ and the current at the pH-sensitive region of the scan was plotted at each xd location. The potential of the substrate electrode was varied from -0.6 to -1.2 V. Over this range of substrate potentials, the rate of H^+ reduction greatly increases, causing a basic change in pH in the vicinity of the substrate even in buffered solutions.^{24–26} This pH gradient is evidenced by in the increasing magnitude of the pH changes in the images of Figure 4. The presence of the weak buffer (0.5 mM HEPES in 150 mM NaCl) keeps pH perturbation to a relatively small distance away from the substrate. While these images are somewhat noisier than those obtained with potentiometric micro-pH sensors, these results highlight the flexibility of the FSCV–SECM technique; by simply changing the applied waveform, a

different type of chemical image was obtained using the same tip in a different solution.

There are, however, some factors that limit the applicability of FSCV to pH imaging in biological systems. First, most biological systems are much more strongly buffered than the solution used for Figure 4. Attempts to detect pH gradients in 5 mM HEPES or the other stronger buffers were unsuccessful because of the relatively low signal-to-noise ratio of the measurement and because of the very small pH changes that occur at higher buffer capacities. Second, we have found the magnitude of the pH response to be highly variable between electrodes and even absent in some cases. This is likely due to differing degrees of oxidation of the carbon surface, as the pH response originates from changes in the background carbon redox waves. Careful selection of a pH-sensitive carbon fiber electrode is thus critical for pH imaging.

Oxygen Imaging at PC12 Cells. PC12 cells are of intense interest in our laboratory because they serve as a model for neuronal growth and development and because they contain releasable stores of the electroactive neurotransmitters dopamine and norepinephrine. As mammalian cells, they consume oxygen during respiration, which results in a local depletion of oxygen in the extracellular solution. Images of changes in oxygen concentration near the cell can be obtained with FSCV–SECM by using the same waveform used for pH measurement in the previous section and plotting the current at the potential for oxygen reduction as a function of xy position. A typical oxygen image at a single PC12 cell is shown in Figure 5B. This image was recorded with the tip positioned 2 μm above the cell, and the current was averaged over the potential range from -1.2 to -1.3 V on the cathodic sweep of the voltammogram. The decrease in current is

(23) Runnels, P. L.; Joseph, J. D.; Logman, M. J.; Wightman, R. M. *Anal. Chem.* **1999**, *71*, 2782–2789.

(24) Horrocks, B. R.; Mirkin, M. V.; Pierce, D. T.; Bard, A. J.; Nagy, G. *Anal. Chem.* **1993**, *65*, 1213–1224.

(25) Klusman, E.; Schultze, J. W. *Electrochim. Acta* **1997**, *42*, 3123–3134.

(26) Wipf, D. O.; Ge, F.; Spaine, T. W.; Baur, J. E. *Anal. Chem.* **2000**, *72*, 4921–4927.

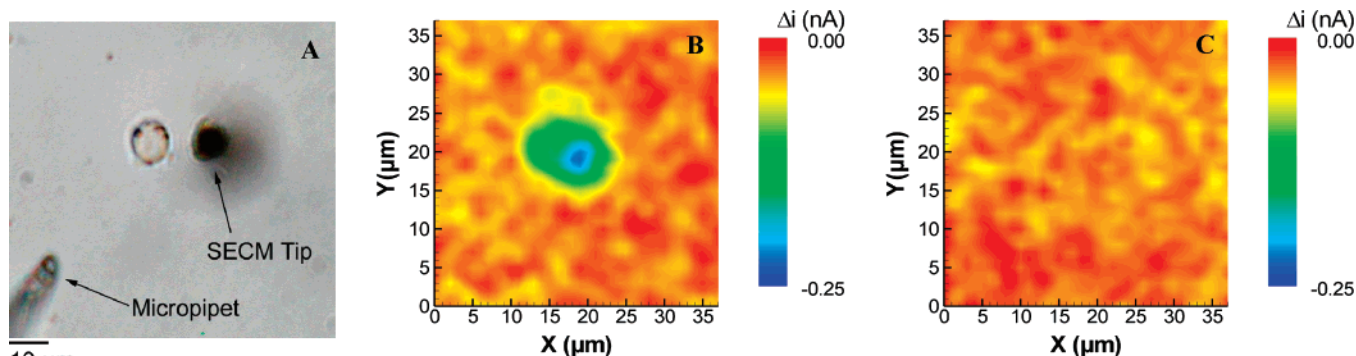


Figure 5. Detection of oxygen consumption by a single PC12 cell by FSCV-SECM. (A) Photomicrograph showing the cell, the 7- μm -diameter carbon fiber electrode used for imaging, and the micropipet used for focal application of NaCN. (B) Change in current measured at the potential for oxygen reduction at the PC12 cell. (C) Image of same region following focal application of 0.8 mM NaCN for 10 min. Images are the average of 14 points in the potential range of -1.20 to -1.30 V on the cathodic sweep of the waveform. The potential applied to the tip consisted of a three-segment waveform (0.0 to $+1.2$ to -1.4 to 0.0 V) having a scan rate of $450 \text{ V}\cdot\text{s}^{-1}$.

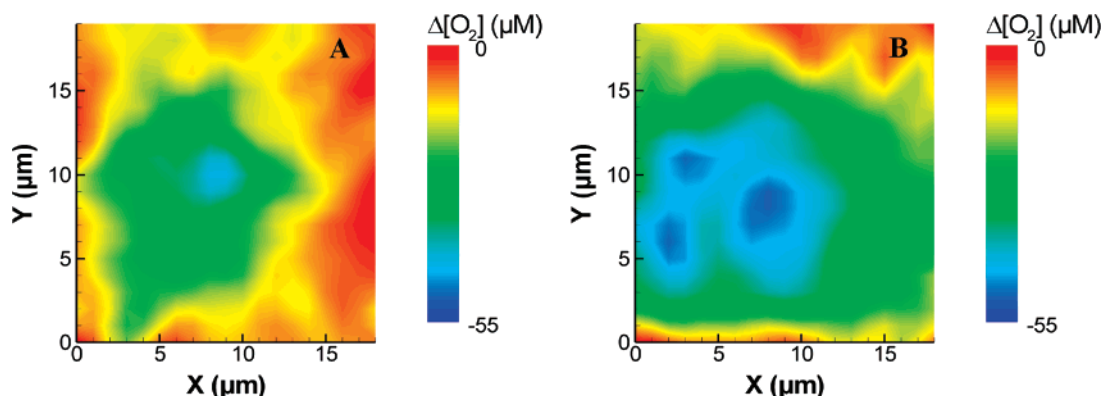


Figure 6. Detection of oxygen consumption by a single PC12 cell (A) before, and (B) immediately following depolarization of the cell by a 10-s focal application 100 mM K^+ . Conditions: Hank's buffer (no mediator), tip voltammetric scan rate $450 \text{ V}\cdot\text{s}^{-1}$. Images are the average of 14 points in the potential range of -1.20 to -1.30 V on the cathodic sweep of the waveform. The potential applied to the tip consisted of a three-segment waveform (0.0 to $+1.2$ to -1.4 to 0.0 V) having a scan rate of $450 \text{ V}\cdot\text{s}^{-1}$.

consistent with a decrease in the local oxygen concentration arising from cell respiration. It should be noted that only *changes* in oxygen concentration can be obtained because only changes in current are measured; information about the absolute concentration of oxygen is contained in the background voltammogram and cannot easily be extracted. To determine whether the image is in fact due to cellular respiration, 0.8 mM NaCN was focally applied for 10 min by pressure ejection from a micropipet and the cell was imaged again (Figure 5C). Since CN^- blocks electron transfer between cytochrome oxidase and oxygen, ceasing cell respiration, the disappearance of the signal strongly suggests that the image of Figure 5B is in fact a local oxygen change resulting from cell respiration.

Similar oxygen images were acquired at a single undifferentiated PC12 cell before and after focal application of 100 mM K^+ (Figure 6). Elevated levels of K^+ depolarize the cell, causing neurotransmitter release and an increased rate of metabolism as the cell restores the transmembrane potential and replenishes vesicular stores of the neurotransmitter. Figure 6A shows the oxygen image immediately before depolarization, and Figure 6B shows the oxygen image immediately following the application of 100 mM K^+ for 20 s. Note that the imaged area is small and the resolution is low so that the images could be recorded quickly (~ 60 s each). These images are plotted on the same color scale to facilitate direct comparison. Before stimulation, a decrease in

oxygen concentration consistent with normal respiration is evident, but following stimulation, there is an appreciable decrease in oxygen concentration, consistent with an increased rate of metabolism. In this experiment, the contour scale allows quantitative comparison of oxygen concentration, as the electrodes were postcalibrated to determine their quantitative response to oxygen.

It should be noted that no signal for dopamine or norepinephrine was detected during these experiments despite the fact that they are detectable using the same voltammetric waveform. This is not surprising considering the quantized, local release of very small quantities of neurotransmitter from the vesicular stores results in very small signals with FSCV.^{27,28} Another factor is that with the moving tip there is a lowered probability that it will be directly over a release site at the moment of exocytosis. Also, the number of release events drops off greatly within seconds of terminating the depolarizing stimulus, further reducing the likelihood of detecting neurotransmitter release.

Chemical Imaging at Macrophages. RAW 264.7 macrophage cells produce an oxidative burst when stimulated with a foreign substance, releasing superoxide, hydrogen peroxide, and other reactive oxygen species.²⁹ Superoxide is not detectable under our present conditions, as it rapidly reacts with water to form oxygen

(27) Heien, M. L. A. V.; Johnson, M. A.; Wightman, R. M. *Anal. Chem.* **2004**, *76*, 5697–5704.

(28) Troyer, K. P.; Wightman, R. M. *J. Biol. Chem.* **2002**, *277*, 29101–29107.

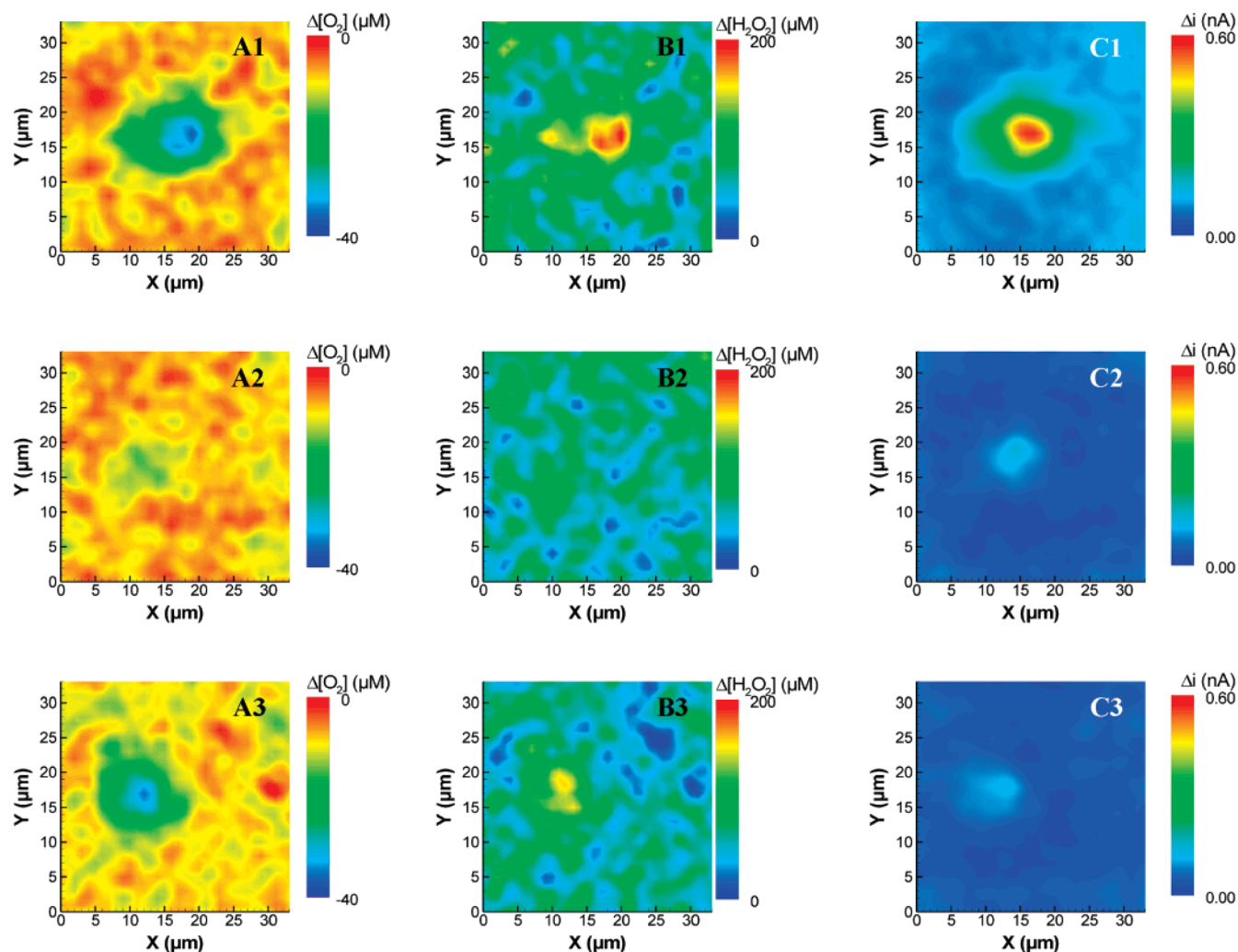


Figure 7. FSCV-SECM images of a single RAW 264.7 macrophage cell following stimulation with zymosan particles (row 1) followed by the addition of 0.3 IU of catalase (row 2) and after washing with fresh Hank's buffer (row 3). Images are shown at (A) the potential for reduction of O_2 (average of 14 points between -1.2 and -1.3 V on cathodic sweep), (B) the potential for H_2O_2 oxidation (average of 12 points between $+1.2$ and $+1.3$ V on the first anodic sweep), and (C) average of -0.45 to -0.55 V on the cathodic sweep. Note that the images in each row were recorded simultaneously. The potential applied to the tip consisted of a three-segment waveform (0.0 to $+1.2$ to -1.4 to 0.0 V) having a scan rate of $450\text{ V}\cdot\text{s}^{-1}$.

and hydrogen peroxide. However, hydrogen peroxide is detectable by the same FSCV waveform used for pH and oxygen measurements, and it should therefore be possible to detect oxygen and hydrogen peroxide *simultaneously* during stimulation of the oxidative burst.

Figure 7 shows a series of images recorded with the tip $\sim 2\text{ }\mu\text{m}$ above the highest point of a single RAW 264.7 cell. The first series of images (A1–C1) was recorded 5 min after stimulation of the oxidative burst by application of zymosan, an insoluble carbohydrate isolated from the cell walls of the yeast *S. cerevisiae* that is known to elicit an immunoresponse from the macrophages. The oxygen image (Figure 7A1) clearly shows a local decrease in oxygen concentration as a result of cell respiration. A small amount of peroxide is detectable, as shown in (B1). Unfortunately, the carbon fiber tip is significantly less sensitive to hydrogen peroxide than oxygen, and thus, the hydrogen peroxide image has a lower signal-to-noise ratio even though its concentration is

greater than that of oxygen (based on postcalibration data). Third, a well-defined image was detected at ~ -0.5 V on the cathodic scan. While the identity of the species producing this signal is not yet known, it is clearly linked to the oxidative burst. This is demonstrated by the second series of images (A2–C2), which were recorded following the addition of 0.3 IU of the enzyme catalase to the culture plate. Catalase catalyzes the disproportionation of hydrogen peroxide to oxygen and water, effectively removing hydrogen peroxide from the extracellular solution. Following addition of catalase, the hydrogen peroxide signal was completely absent (B2), and the signal at -0.5 V also was nearly eliminated (C2). At the same time, the oxygen image (A2) is also nearly eliminated. This is not surprising, as the oxygen formed by the enzymatic disproportionation of hydrogen peroxide will increase the local oxygen concentration, effectively counteracting the oxygen gradient produced by respiration.

To ensure that these changes did not arise from the death of the macrophage, the buffer containing the catalase and zymosan was removed and replaced with fresh Hank's buffer (containing

(29) Hampton, M. B.; Kettle, A. J.; Winterbourn, C. C. *Blood* **1998**, *92*, 3007–3017.

no zymosan). These data are shown in the third series of images (A3–C3). The oxygen image (A3) shows that the local depletion of oxygen is nearly restored to its original value, indicating that the cell is still viable. There appears to be a small hydrogen peroxide signal (B3) and a small signal for the unknown species (C3). The origin of these signals is unclear, but might reflect some residual oxidative activity due to incomplete removal of the zymosan. One strength of SECM is that the tip can be held stationary at a location of interest and chemical events at that location can be monitored as a function of time. Using this type of approach should help to elucidate the origin of the signal in Figure 7C1–C3; such experiments are underway. Nonetheless, this experiment shows that multiple species are detectable using FSCV–SECM and that chemical images can be extracted by plotting current as a function of tip location at the appropriate potential.

CONCLUSIONS

These results demonstrate that FSCV–SECM is a useful technique for chemical imaging of species with micrometer resolution near an active biological substrate and that simultaneous detection of analytes having differing redox potentials is possible. Because the thickness of the diffusion layer with FSCV is so small, these measurements can be made without significant diffusional interaction between the tip and substrate, especially when higher voltammetric scan rates are used. As a result, the

chemical images are not prone to perturbations due to substrate topography.

To further develop the technique for applications in biological systems it will be necessary to improve the signal-to-noise ratio, especially at faster voltammetric scan rates, by using a lower noise potentiostat and improving the data acquisition software to include digital filtering. Additionally, it would be advantageous to incorporate a constant-distance technique so that the chemical images are completely independent of substrate topography. While the constant-height imaging approach used in this work can be used for samples with low relief, it is difficult to apply to biological substrates with high relief.¹² However, by thoughtful solution of these problems, FSCV–SECM has the potential to greatly expand the amount of information produced by a single SECM experiment, and it will likely find applications in many complex systems.

ACKNOWLEDGMENT

The authors thank Dr. David O. Wipf for assistance with hardware and software and Dr. C. Frank Shaw for providing the RAW 264.7 macrophage cells. This work was supported by the National Institutes of Health (R15 NS050103-01).

Received for review June 1, 2007. Accepted July 11, 2007.
AC071155T